

## Regular article

## $\gamma'$ precipitates with a twin orientation relationship to their hosting grain in a $\gamma$ - $\gamma'$ nickel-based superalloy



Suzanne Vernier<sup>a,b,\*</sup>, Jean-Michel Franchet<sup>b</sup>, Christian Dumont<sup>c</sup>, Philippe Vennéguès<sup>d</sup>, Nathalie Bozzolo<sup>a</sup>

<sup>a</sup> MINES ParisTech, PSL – Research University, CEMEF – Centre de mise en forme des matériaux, CNRS UMR 7635, 1 rue Claude Daunesse, 06904 Sophia Antipolis, France

<sup>b</sup> Safran SA, Safran Tech – Materials & Process Department, 1 Rue Geneviève Aubé, 78114 Magny-les-Hameaux, France

<sup>c</sup> Aubert & Duval, Département R&D transformations, BPI, 63 770 Les Ancizes, France

<sup>d</sup> CRHEA-CNRS, UPR 10, rue Bernard Grégory, 06560 Valbonne, France

## ARTICLE INFO

## Article history:

Received 8 March 2018

Received in revised form 21 April 2018

Accepted 22 April 2018

Available online xxxx

## Keywords:

Gamma – gamma prime nickel-based superalloy

Interphase boundary

Twin boundary

Recrystallization

## ABSTRACT

In a polycrystalline  $\gamma$ - $\gamma'$  nickel-based superalloy,  $\gamma'$  precipitates with a close-to-twin orientation relationship to their surrounding matrix (named T-type precipitates) are found in recrystallized grains located near specific unrecrystallized grains (named recovered grains). This type of  $\gamma/\gamma'$  interface has not been reported in literature before. Inherited from the ingot conversion process, recovered grains are characterized by a high density of micrometric and close-to-coherent  $\gamma'$  precipitates. Resulting from the interaction of the recrystallization front with the latter precipitates, the T-type precipitates appear to form onto the recrystallization front. The present paper details the crystallographic characteristics of the T-type precipitates.

© 2018 Published by Elsevier Ltd on behalf of Acta Materialia Inc.

Polycrystalline  $\gamma$ - $\gamma'$  nickel-based superalloys are commonly used to manufacture aircraft engine rotative parts due to their good mechanical behavior at high temperature (tensile, fatigue, creep resistance) [1]. Parts are usually derived from cast ingots through forging sequences [2,3]. They are made of a  $\gamma$  matrix in which  $\gamma'$  precipitates of various sizes are distributed. Both  $\gamma$  and  $\gamma'$  phases have a cubic structure but, while the  $\gamma$  phase is a Face Centered Cubic (FCC) non-ordered solid solution, the  $\gamma'$ -Ni<sub>3</sub>(Al,Ti) phase has a L1<sub>2</sub> ordered structure. Yet, the mechanical properties of the alloy do not only depend on the size and spatial distribution of the precipitates [4], but also on the  $\gamma/\gamma'$  interface characteristics [5,6]. Indeed,  $\gamma'$  precipitates are reported in literature as coherent, semi-coherent or incoherent to their surrounding matrix [7]. Coherency means that the  $\gamma$  and  $\gamma'$  crystal lattices perfectly coincide at the  $\gamma/\gamma'$  interface. This is made possible by a low lattice parameter mismatch between the  $\gamma$  and  $\gamma'$  phases [8]. Coherent  $\gamma/\gamma'$  interfaces have very low energies [9,10]. However, if some misfit dislocations pile up at the  $\gamma/\gamma'$  interface, the lattice matching is only partial and the interface is semi-coherent [7]. Semi-coherency occurs when external stresses (high temperature plastic deformation) or internal stresses (e.g. induced by long aging treatments leading to particle coarsening) generate dislocation loops which are incorporated into the  $\gamma/\gamma'$

interface as misfit dislocations [11]. Finally, when there is no crystal lattice matching, the  $\gamma/\gamma'$  interface is incoherent and has a high energy [9]. Secondary  $\gamma'$  precipitates, which form during the cooling stages of the forming process, are coherent with a cube-cube orientation relationship: they evolve from spheres to {100} bounded cubes as their size and/or the lattice misfit increase [12]. On the other hand, derived from the as-cast microstructure and high temperature billet forging sequences, primary  $\gamma'$  precipitates are usually incoherent with no special orientation relationship, except in the case of heteroepitaxial recrystallization where primary precipitates are found coherent with an orientation very close to that of their surrounding matrix [13–15]. The present work points out another type of  $\gamma/\gamma'$  interface which, to the best knowledge of the authors, has not been reported in literature before:  $\gamma'$  precipitates with a close-to-twin orientation relationship to their surrounding  $\gamma$  matrix have been evidenced. Those precipitates will be called T-type precipitates below. Close-to-twin means that the two  $\gamma$  and  $\gamma'$  cubic crystallographic cells are related by a misorientation close to, but a few degrees off, the theoretical 60° rotation around a common  $\langle 111 \rangle$  axis. The  $\Delta\theta$  tolerance which has been used to detect the T-type precipitates applies both to the 60° rotation angle and the  $\langle 111 \rangle$  rotation axis, and amounts to 8.66° following Brandon's criterion for FCC twin boundaries [16]. T-type precipitates fall into this 8.66° tolerance and only very few of them strictly fulfills the perfect 60° $\langle 111 \rangle$ , which implies that the considered  $\gamma/\gamma'$  interfaces must be regarded as incoherent. T-type precipitates are found in some recrystallized grains next to unrecrystallized grains characterized by a high density of micrometric

\* Corresponding author at: MINES ParisTech, PSL – Research University, CEMEF – Centre de mise en forme des matériaux, CNRS UMR 7635, 1 rue Claude Daunesse, 06904 Sophia Antipolis, France.

E-mail address: [suzanne.vernier@mines-paristech.fr](mailto:suzanne.vernier@mines-paristech.fr) (S. Vernier).

close-to-coherent precipitates and called recovered grains. The present paper details the crystallographic characteristics of the T-type precipitates.

The AD730™ nickel-based superalloy whose composition is Ni-15.7Cr-8.5Co-4.0Fe-3.4Ti-3.1Mo-2.7W-2.25Al-1.1Nb-0.01B-0.015C-0.03Zr (wt%) [17] is studied. Samples are cut out from an AD730™ billet which contains elongated unrecrystallized grains typical of many cast-and-wrought heavily-alloyed  $\gamma/\gamma'$  nickel-based superalloys [18–20]. These grains are inherited from the ingot conversion process and characterized by a high density of intragranular precipitates. The samples were compressed at a sub-solvus temperature then solution-treated for 4 h at 1080 °C. The  $\gamma'$  solvus temperature of the alloy is about 1110 °C. Longitudinal sample cross-sections were ground with Si papers and polished with diamond suspensions down to 1  $\mu\text{m}$ . Finally, to obtain a suitable surface quality for EBSD, samples were polished either by electropolishing ( $\text{CH}_3\text{OH}$ -10% $\text{HClO}_4$ ) or with a 0.02  $\mu\text{m}$  colloidal silica solution on a vibratory machine. Some samples also underwent a deeper electrolytic etching ( $\text{H}_2\text{SO}_4$ -42% $\text{HNO}_3$ -13% $\text{H}_3\text{PO}_4$ ) to selectively dissolve the matrix and bring the  $\gamma'$  precipitates more into relief. SEM observations were carried out with a Zeiss Supra40 FEG-SEM operated at 15 kV. The microscope is equipped with the QUANTAX EDS/EBSD system, from the Bruker Company, which is composed of an EDS XFlash 5030 detector and an  $e^-$  Flash<sup>HR</sup> EBSD detector, both controlled by the ESPRIT® software package. Some EBSD data post-treatments were performed using MTEX, a freely available Matlab toolbox [21]. A TEM thin foil was lifted out of a region of interest using a Zeiss Crossbeam 550 FIB-SEM, equipped with an Oxford Instruments Symmetry EBSD detector which was used to perform Transmission Kikuchi Diffraction

analyses (TKD) at 30 kV. Finally, TEM observations were performed with a JEOL 2100 FEG-TEM operated at 200 kV.

The samples present some areas where the recrystallized grain size is much larger than anywhere else. Those large recrystallized grains are located next to elongated unrecrystallized grains (Fig. 1). These unrecrystallized grains show a high density of micrometric close-to-coherent precipitates and quite well-defined recovery cells; they will henceforth be called recovered grains. Here, the large recrystallized grains, which appeared during the solution treatment, have extensively grown inside the recovered grain to consume the stored strain energy. The large recrystallized grains exhibit numerous intragranular particles, many of them having a twin orientation relationship to their hosting grain within the tolerance given by Brandon's criterion (white boundaries in Fig. 1). These particles with a close-to-twin orientation relationship, and called T-type precipitates in the following, were proved to be  $\gamma'$  precipitates considering two points. First, their chemical composition is rich in Ni, Ti and Al. It is close to that of the primary precipitates and even closer to that of the precipitates inside the recovered grains (Table 1). The fact that primary precipitates most likely formed at higher temperature than the precipitates of the recovered grains can account for the slight differences in composition. Then, the TEM diffraction pattern of a T-type precipitate shows superstructure spots, confirming a  $L1_2$  ordered structure whose cubic lattice parameter is very close to that of the non-ordered matrix (Fig. 4).

Several arguments demonstrate that T-type precipitates are not the precipitates of the recovered grain which have been simply bypassed by the recrystallization front. They do originate from a specific mechanism and the T-type precipitate visible on the recrystallization front in Fig. 2.b

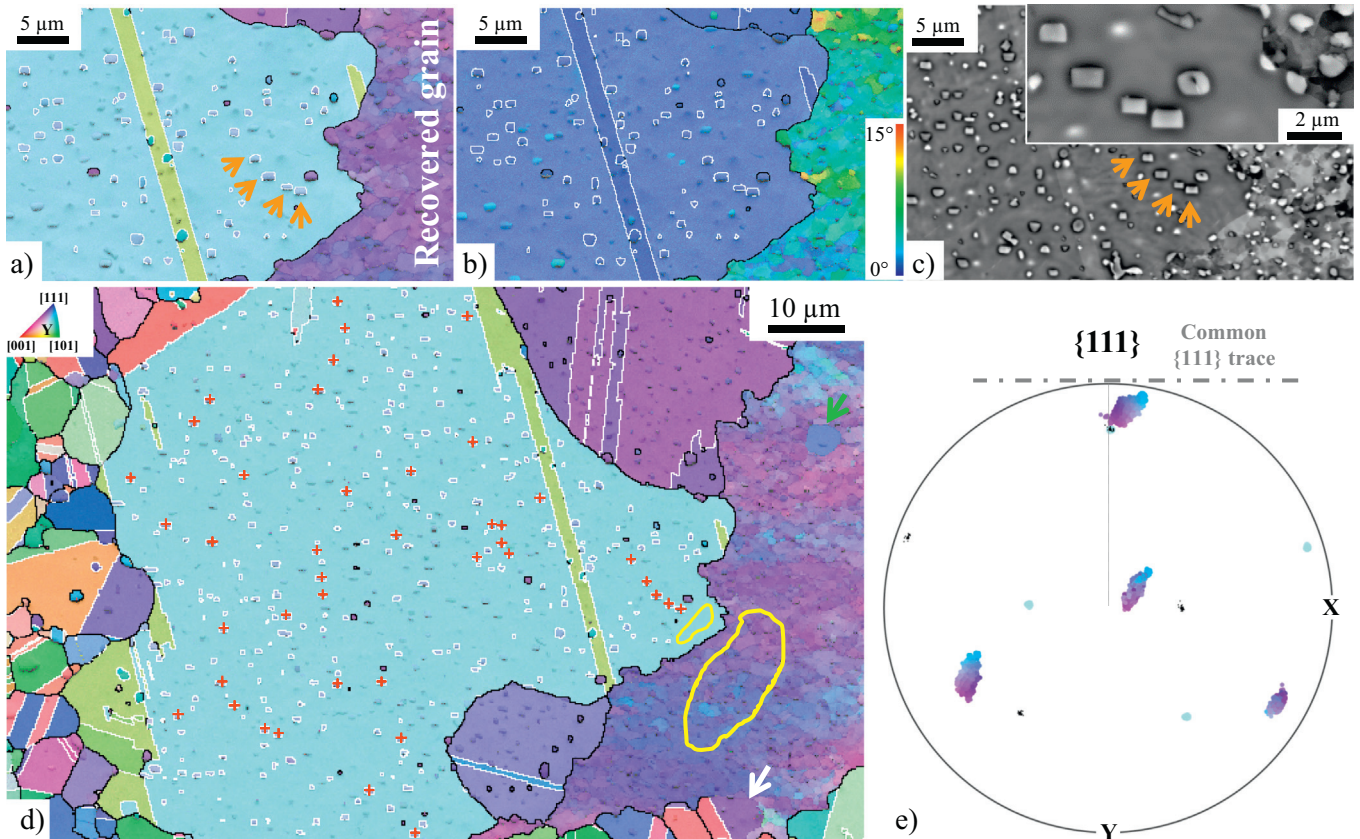


**Fig. 1.**  $\gamma'$  precipitates with a twin orientation relationship to the matrix observed after static recrystallization. a) and d) Orientation overlaid on the band contrast map, grain boundaries plotted black (misorientation angle threshold: 10°) and twin boundaries (60° $\{111\}$  with 8.66° tolerance, following Brandon's criterion [16]) plotted white. The green and white arrows highlight HERX and CRX respectively. b) Misorientation angle to the mean grain orientation overlaid on the band contrast map. c) Backscattered electron images, where  $\gamma'$  precipitates appear bright despite their lower atomic number because of topographic effects induced by electropolishing. Orange arrows show examples of  $\gamma'$  precipitates with a twin orientation relationship to the matrix. e)  $\{111\}$  pole figure. Orientations of T-type precipitates (red crosses in d)) are plotted black; those of the matrix and the recovered grain (yellow selections in d)) are plotted with the same color as displayed in d). The dashed line is the  $\{111\}$  plane trace common to the T-type precipitates and the matrix. (For interpretation of the references to color in this figure legend, the reader is referred to the web version of this article.)

Download English Version:

<https://daneshyari.com/en/article/7910404>

Download Persian Version:

<https://daneshyari.com/article/7910404>

[Daneshyari.com](https://daneshyari.com)